MRS Communications (2017), 7, 658–663
© Materials Research Society, 2017
doi:10.1557/mrc.2017.38

MRS Communications

Research Letter

Morphological stability during electrodeposition

Raúl A. Enrique, Stephen DeWitt, and **Katsuyo Thornton,** Joint Center for Energy Research Storage, and Department of Materials Science and Engineering, University of Michigan, Ann Arbor, Michigan 48109, USA

Address all Correspondence to Katsuyo Thornton at **kthorn@umich.edu**

(Received 23 January 2017; accepted 31 May 2017)

Abstract

The uniform electrodeposition of certain materials, such as Li metal, remains elusive because the mechanisms controlling growth instability are not fully understood. To determine the conditions that lead to either stable or unstable deposition, we develop a phase-field model for the growth of multiple deposits in a binary electrolyte and examine the behavior as the kinetic parameters are varied. We find that the second Damköhler number, defined as the ratio between the reaction and the mass transfer fluxes, is an indicator of deposition instability. Our results suggest that controlling reaction kinetics and initial roughness are essential in achieving stable electrodeposition.

Electrodeposition is a synthesis method with numerous applications, such as surface coating and plating and fabrication of microelectronics.[1] It also occurs during operation in some systems such as rechargeable batteries. Electrodeposition often results in the formation of unstable morphologies such as dendrites, with characteristic length scales ranging from tens of nanometers to tens of microns. While these instabilities can be exploited to synthesize nanostructures, in many applications including batteries, dendrite formation must be avoided. In fact, dendrite formation during charging remains one of the major hurdles for the development of lithium metal batteries.

Solidification and electrodeposition share one common feature: in both cases, the growth of the crystal is influenced by diffusion (of solute or latent heat in solidification and ions in electrodeposition). Therefore, models developed for solidification have been applied to describe unstable electrodeposition. For example, Barton and Bockris[2] introduced a model of dendritic growth based on the difference between the diffusion fluxes associated with planar and spherical geometries. Although this is a valuable first approximation,[3,4] this type of analysis does not rigorously incorporate the coupling between ionic diffusion, electrostatics, and the kinetics of electrochemical reactions.

In addition to the growth instabilities that arise from diffusion, the electrostatic potential, which is also governed by a Laplace-type equation, has been identified as a possible source of unstable deposition.[5] According to electrostatics, an equipotential surface induces a localized enhancement of the electric field around protuberances inversely proportional to the local radius of curvature.[6] This local enhancement, called the 'lightning rod' effect, has been used to explain the preferred growth at dendrite tips.[5]

The deposition flux during electrodeposition is governed by the electrochemical reaction rate, for which the Butler–Volmer equation is often employed to describe the nonlinear relationship between the flux and the value of electrostatic potential. A linear stability analysis of electrodeposition on flat electrodes yields finite, positive growth rates for long wavelength perturbations,[7] suggesting that morphological instabilities prevail for all applied currents. However, such analysis does not account for the nonlinearities linking the evolution of the ionic concentration, the Butler–Volmer reaction kinetics, the electrostatic potential, and the complex geometry of the evolving front; in addition, incipient instabilities might be overrun by the growing deposits. Indeed, experiments have shown that stable growth is possible for certain metals such as Mg,[8] while instabilities are frequently observed in other metals like Li.[9]

The strong coupling of electrostatics and ion migration via nonlinear reaction kinetics at an evolving, and possibly complex, surface makes the phase-field method a well-suited tool to study electrodeposition at the micrometer length scale. Most studies utilizing this approach have focused on the conditions for unstable growth,[10–12] but there are also works that performed simulations of the stable electrodeposition of Mg.[8] The objective of the present work is to identify the conditions that drive the transition from stable to unstable growth.

We consider a half cell, where a material is being electrodeposited on a substrate immersed in a binary electrolyte.[8,13] Each region of the simulation domain is defined by a field variable similar to a phase field order parameter that takes the value one inside and zero outside of each subdomain: ψ_s indicates the substrate, ψ_1 the electrolyte, and η_i each grain of the deposit, where the index i ranges from 1 to p. The order parameter of the substrate ψ_s is assumed to be constant in time. The

https://doi.org/10.1557/mrc.2017.38 Published online by Cambridge University Press

evolution equations for the remaining order parameters are derived from a free-energy functional $\mathcal{F}$ proposed for modeling grain growth in polycrystalline solids.[14] The governing equation for η_i is based on the Cahn–Hilliard equation,[15] which ensures mass conservation. Since electrochemical reaction only occurs at the surface of the deposit exposed to the electrolyte, we express the normal unit vector of the reacting surfaces in terms of the gradient of ψ_l. Thus, the evolution equation for η_i is given by[8]

$$\frac{\partial \eta_i}{\partial t} = \nabla M_{\eta_i} \nabla \frac{\delta \mathcal{F}}{\delta \eta_i} - v\left(\frac{\nabla \psi_l}{|\nabla \psi_l|} \cdot \nabla \eta_i\right). \quad (1)$$

Assuming that currents arising from non-faradaic processes can be neglected, the normal velocity of the interface is related to the reaction current density i_{rxn} via $v = i_{rxn}/(z_+ F C_s)$, in which C_s is the number density of atoms in the deposits, C_l the concentration of ions in the electrolyte, z_+ the charge number, and F the Faraday constant. As the deposit grows, the electrolyte is displaced; we employ the Allen–Cahn equation[16] for the evolution of ψ_l,

$$\frac{\partial \psi_l}{\partial t} = -L_{\psi_l} \frac{\delta \mathcal{F}}{\delta \psi_l}. \quad (2)$$

For the scope of the present paper, we make the approximation of a uniform concentration of ions, corresponding to a well-stirred electrolyte, or assuming short times compared with diffusion time scales. While conducting the calculations presented in this work we also performed preliminary simulations of electrodeposition that accounted for the evolution of the concentration of ions, and we did not observe that ionic diffusion could be a source of unstable growth before Sand's time (the characteristic time until the electrolyte is depleted near the electrode). Even though depletion can be a source of instabilities for highly driven systems due to the appearance of space-charge regions,[17,18] unstable growth has also been commonly observed before Sand's time.[9] Therefore, our study is applicable to the onset of unstable growth during the early stages of the electrodeposition process.

We obtain the electrostatic potential by solving the continuity equation for the current, $\nabla \cdot i = 0$, along with electroneutrality, which yields[8,13]

$$z_+ C_l F \nabla\left[(z_+ D_+ - z_- D_-)\frac{F}{RT}\nabla \phi\right] = 0, \quad (3)$$

where ϕ is the electrostatic potential, and we have replaced mobilities with diffusivities by making use of Einstein's relation. D_+ and D_- are the cation and anion diffusivities, z_+ and z_- are the corresponding charge numbers, R is the gas constant, and T is the temperature. Here, we note that the ionic conductivity can be written as $\kappa = z_+ C_l F^2 (z_+ D_+ - z_- D_-)/RT$.

The smoothed boundary method[19] is utilized to combine the governing equation with the associated boundary conditions on the evolving domain of the electrolyte. Thus, Eq. (3) is reformulated as

$$\nabla \psi_l \left[(z_+ D_+ - z_- D_-)\frac{C_l F}{RT}\nabla \phi\right] + |\nabla \psi_l| \frac{i_{rxn}}{z_+ F} = 0. \quad (4)$$

Because the substrate and the deposit are both metallic solids, their electrostatic potential is assumed to be uniform, with a value denoted by ϕ_w. Potential drops within the substrate and deposit are therefore neglected in this work, which is a good approximation for the geometries we consider. Deposition is then driven by the overpotential $\phi - \phi_w$, and the reaction current density i_{rxn} is given by the Butler–Volmer equation,[1]

$$i_{rxn} = i_0 (e^{\beta z_+ F(\phi - \phi_w)/RT} - e^{-(1-\beta) z_+ F(\phi - \phi_w)/RT}), \quad (5)$$

where i_0 is the exchange current density and β is the symmetry factor. Combining Eqs. (4) and (5), a dimensional analysis with $\tilde{\phi} = (\phi - \phi_w)/\phi^*$ and $\tilde{x} = x/L^*$ yields characteristic units for the potential and length scale: $\phi^* = RT/F$ and $L^* = ((z_+ D_+ - z_- D_-) z_+ F C_l)/i_0$, which depend solely on the material parameters and not on the configuration of the electrodeposition setup.

Electrodeposition as described above is controlled by ionic migration and reaction kinetics. The suitable dimensionless number is then the second Damköhler number, defined to measure the relative magnitude of the chemical reaction flux to the mass migration flux, $Da_{II} \propto i_0/\kappa$.[20] Given the length scale L associated with the geometry of the electrode and its features, we write

$$Da_{II} = \frac{F}{RT}\frac{i_0 L}{\kappa} = \frac{L}{L^*}. \quad (6)$$

Da_{II} may therefore be reinterpreted as the ratio between the length scale L of the geometry to the characteristic length scale L^* given by the material parameters.

Our simulations indicate that, within the model presented here, there are two main conditions leading to unstable growth. One is linked to large exchange current densities, as measured by Da_{II}, and the other related to very large deposition currents.[5] To examine each of these instabilities, we proceed by studying the reaction rates on the surface of a model 'dendrite,' a single columnar deposit with a hemispherical tip. The details of the model, along with the numerical methods used and the material parameters (chosen to correspond to typical values for Li electrodeposition during battery operation) are summarized in the Supplementary Material.

Figure 1 shows the calculated reaction rates on the dendrite's surface as i_0 is varied from 4×10 to 4×10^3 mA/cm^2. Note that values calculated from experimental data assuming uniform deposition are in the range $0.1 \sim 10$ mA/cm^2.[21] However, due to the experimental difficulties in achieving stable Li electrodeposition, reliable exchange current density measurements are scarce; these values are likely underestimated, considering that unstable deposition is highly localized. The distribution of the reaction current density is indicated by the

https://doi.org/10.1557/mrc.2017.38 Published online by Cambridge University Press

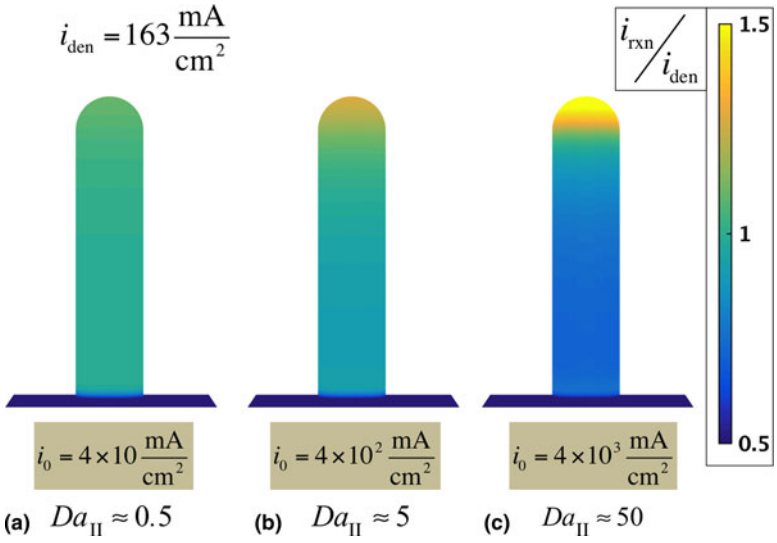


Fig. 1. Non-uniform electrodeposition produced by high exchange current densities. Side view of a single dome-capped columnar 'dendrite' with 1 μm radius and 9 μmheight placed on a 30 μm square substrate. A 10 mA/cm^2 current density is applied over the total area, resulting in an averaged current density of i_{den} = 163 mA/cm^2 on the deposit; the substrate is assumed to be inert. Results at t = 0 s show enhancement of the reaction current i_{rxn} at the tip of the deposit as i_0 is increased from (a) $i_0 = 4 \times 10$ mA/cm^2 to (b) $i_0 = 4 \times 10^2$ mA/cm^2 to (c) $i_0 = 4 \times 10^3$ mA/cm^2. The second Damköhler number is evaluated from $Da_{II} = (F/RT)(i_0 L/\kappa)$ with L = 9 μm.

color on the surface, which corresponds to the ratio between the local reaction rate i_{rxn} and the average current density over the dendrite's surface, i_{den}. Taking the height of the column as the length scale L, $Da_{II} = L/L^*$ is evaluated, which varies by two orders of magnitude from 0.5 (Fig. 1(a)) to 50 (Fig. 1(c)). Figure 1(a), with $Da_{II} \approx 0.5$, exhibits nearly uniform deposition rates, indicating that the columnar shape itself, with a high curvature dome capping a flat-sided cylinder, does not always lead to unstable growth. Enhancement of the reaction rates due to curvature is not observed, and therefore the 'lightning rod' effect does not necessarily occur under the Butler–Volmer reaction kinetics. However, when the column height is larger than the characteristic length scale, i.e., for greater values of Da_{II}, we observe a relative increase of the reaction rate at the dendrite tip, which would lead to unstable growth. It should be noted that, for the parameters in these calculations, the nondimensional potential, and therefore the arguments of the exponential terms in the Butler–Volmer equation, are much smaller than one, becoming even smaller as i_0 is increased. Therefore, the instability stemming from large exchange current densities is not influenced by the exponent in the Butler–Volmer equation, and this behavior would also occur in the linearized formulation of the equation.[12] Thus, if present, this type of instability would not be mitigated by lowering the deposition current. Experimentally, a correlation between lower exchange current densities — produced by the inclusion of additives — and stable electrodeposition has been observed for zinc metal.[22]

The applicability of the Damköhler number in determining the condition of stability can be justified from the general features of the electrostatic potential in these simulations, as follows. We find that during electrodeposition, the overpotential variations on the surface of the deposit depend on the height difference along the general direction of the electric field rather than on the differences in curvature. Furthermore, we observe that such variation in potential is comparable in magnitude with the potential drop over a similar length scale in the electrolyte. With L representing the length scale of features of the deposit, the variation of potential along a distance L is approximately given by $\Delta\phi = i_{nom} L/\kappa$, where i_{nom} is the nominal current density defined as the average deposition current density in the electrolyte far from the deposit. Whether this potential difference is significant enough to trigger instabilities depends on the corresponding variation in reaction current density, which can be estimated from the Butler–Volmer equation,

$$\Delta i_{rxn} = \frac{di_{rxn}}{d\phi}\Delta\phi \approx i_0 \frac{z\beta F}{RT}\Delta\phi = i_0 \frac{z\beta F}{RT}\frac{i_{nom}L}{\kappa}. \quad (7)$$

The tendency for non-uniform deposition can be characterized by the ratio between the variations in reaction current density to the average deposition current density,

$$\frac{\Delta i_{rxn}}{i_{nom}} \approx i_0 \frac{z\beta F}{RT}\frac{L}{\kappa} = \beta Da_{II}. \quad (8)$$

Therefore, within an order of magnitude, Da_{II} serves as a measure of growth instability. Similarly, the condition of stability can also be expressed in terms of the Wagner number, $W = (d\phi/di)(\kappa/L)$,[1,23] in the form $\Delta i_{rxn}/i_{nom} \approx 1/W$.

Generally, systems governed by Laplace's equation, such as solidifying solid–liquid mixtures, are susceptible to unstable growth due to the convergence of gradient lines towards protuberances when the surface is set at a constant-value boundary

https://doi.org/10.1557/mrc.2017.38 Published online by Cambridge University Press

condition,[24] analogous to an equipotential surface. However, because the Butler–Volmer kinetics makes the flux a function of the potential, morphological evolution during electrodeposition exhibits some unique features, distinct from those of solidification. The Butler–Volmer kinetics dictates a uniform reaction rate on a surface with a constant overpotential, therefore not allowing for 'lightning rod' curvature effects. Our simulations demonstrate that the electrostatic potential at the deposit's surface varies to satisfy the galvanostatic boundary condition. The magnitude of these potential variations may trigger instabilities only if they are large enough to produce significant differences in reaction rates. In all our simulations, we observe a higher reaction rate on hills compared with valleys, in agreement with linear stability analysis that predicts morphological instabilities for all values of applied current.[7] However, only when the value of L/L^* is large, this non-uniform growth is significant enough to induce instabilities.

Even for low Damköhler numbers, the nonlinearity of the Butler–Volmer equation can contribute to unstable growth at large overpotentials, which occurs at high deposition current densities relative to i_0. Figure 2 illustrates this scenario, where we take the setup from Fig. 1 and, while fixing i_0 at a value corresponding to $Da_{II} \approx 0.05$, we apply nominal currents of 1 mA/cm^2 (Fig. 2(a)) and 100 mA/cm^2(Fig. 2(b)). As in Fig. 1, the color indicates the ratio of the reaction current density to the reaction current density averaged over the dendrite surface. It can be observed that the higher-current case results in an increase of the relative reaction rate at the tip of the column, indicating that sufficiently high current densities would also induce unstable growth. In order to observe non-uniform reaction rates, a very high current density is assumed in this

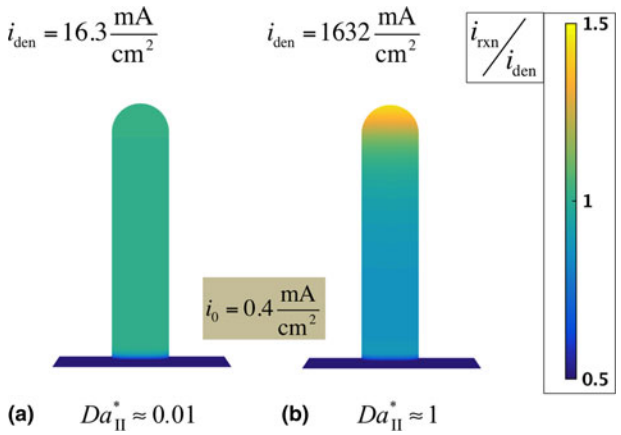


Fig. 2. Non-uniform reaction rate caused by large deposition currents. Side view of a single hemispherical columnar 'dendrite' with 1 μm radius and 9 μmheight on a 30 μm square substrate and an exchange current density of i_0 = 0.4 mA/cm^2. Nominal current densities of (a) 1 mA/cm^2 and (b) 100 mA/cm^2 are applied over the total simulation area, resulting in averaged current densities of (a) i_{den} = 16.3 mA/cm^2 and (b) i_{den} = 1632 mA/cm^2 on the deposits. Results at t = 0 s show enhancement of the reaction current i_{rxn} at the tip of the deposit for higher currents. The modified Damköhler number is computed from $Da_{II}^* = (F/RT)(i_{nom}L/\kappa)$ with L = 9 μm.

calculation, but it should be noted that it is not an unrealistic value, as local current densities of 100–400 mA/cm^2 have been estimated at dendrite tips during Li electrodeposition.[25]

In principle, lowering the average deposition current or increasing the reaction surface area can mitigate this type of instability. For this case of large applied currents, we have also observed that variations in potential on the surface of the deposit depend mainly on the height difference and are approximately proportional to $\Delta\phi = i_{nom}\, L/\kappa$. Noting that, for this case, only the deposition term of the Butler–Volmer equation is significant, one can characterize reaction inhomogeneities by the ratio between the currents of peaks compared with valleys:

$$\frac{i_{peak}}{i_{valley}} \approx \exp(Fz_+\Delta\phi/RT) = \exp(z_+\beta F i_{nom}/RT\kappa).$$

Thus, for large currents, stability is controlled by a Damköhler-like nondimensional number that still has the deposit surface roughness as the characteristic length scale but replaces the exchange current density with the nominal deposition current, $Da_{II}^* = (F/RT)(i_{nom}L/\kappa)$.

A deposit morphology that would more closely represent electrodeposition onto an inert conductive electrode, with an initial distribution of small seed grains is shown in Fig. 3. On a 24 × 28 μm substrate, we place 12 nuclei with random radii in the range 0.8 ∼ 3.0 μm in a triangular array. An average current of 10 mA/cm^2 is applied for 400 s with i_0 = 0.4 mA/cm^2 (Fig. 3(a)) and $i_0 = 4 \times 10^2$ mA/cm^2 (Fig. 3(b)). For a low exchange current density (Fig. 3(a)), nuclei grow nearly uniformly and merge towards a compact film of columnar deposits like those reported by Zhang *et al.*[26] In contrast, a high exchange current causes nuclei to grow preferentially at the tip (Fig. 3(b)), resulting in a growth morphology similar to that recently reported by *in situ* electron microscopy by Mehdi *et al.*[27] and Leenheer *et al.*,[28] with deposits taking an elongated 'light bulb' shape.

Recently, Cogswell[29] reported a similar analysis of electrodeposition using phase field modeling. Although the model construction and the simulation methods are different (for instance, the present work includes 3D simulations of multigrain material), Cogswell also determines that the Damköhler number is a parameter that governs growth stability. However, the physical parameters that enter into the Damköhler number expressions are different, as well as the manner in which the expressions are constructed. In this work, we derive the Damköhler number as a measure of instability by linearizing the Butler–Volmer equation (Eqs. (7) and (8)), while Cogswell makes use of a purely dimensional argument, leading to an incorrect choice of the parameters that enter into the analysis. For example, Cogswell's expression is inversely proportional to C_s (instead of C_l) and takes the electrode separation as the relevant length scale L (instead of the length scale associated with surface roughness). We propose that our expression for the Damköhler number is a direct indication of morphological stability during electrodeposition, as we find that uneven

https://doi.org/10.1557/mrc.2017.38 Published online by Cambridge University Press

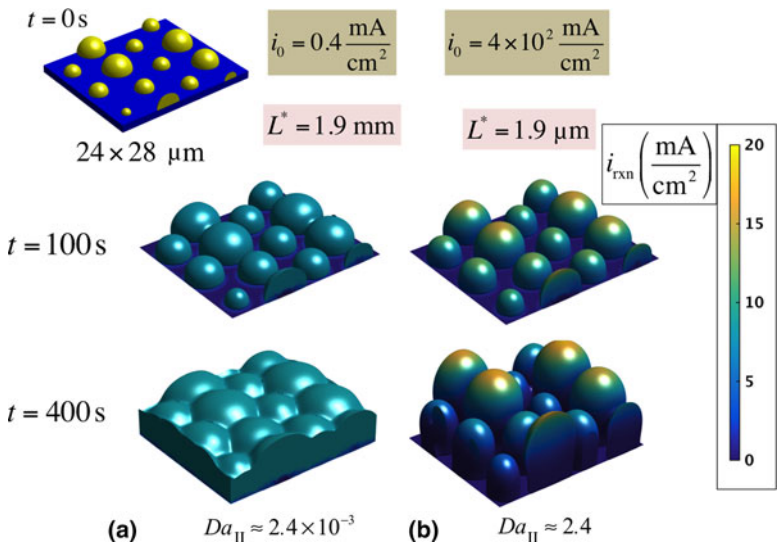


Fig. 3. Morphological evolution for a distribution of deposits for low and high values of i_0. Galvanostatic electrodeposition at 10 mA/cm^2, starting from a triangular array of nuclei with random radii in the range 0.8–3.0 μm and average separation of $L = 4.7$ μm, with exchange currents of (a) $i_0 = 0.4$ mA/cm^2 and (b) $i_0 = 4 \times 10^2$ mA/cm^2. Higher exchange current densities lead to the formation of unstable deposits. The second Damköhler number is evaluated from $Da_{II} = (F/RT)(i_0 L/\kappa)$ with $L = 4.7$ μm.

growth is not affected by the inter-electrode spacing, but rather depends on the magnitude of the gradient of the potential relative to the exchange current density, which leads to an expression inversely proportional to C_l. Also, we find that the relevant length scale for L should be given by that associated with the surface roughness, whether it originates from uneven reaction rates, nucleation events, or non-uniformly distributed catalysts, as this increases the difference in the deposition current density at protrusions compared with other regions.

It is important to note that we have implicitly assumed uniform kinetic properties at the deposit/electrolyte interface. Therefore, the model described here do not account for dendritic structures that would result from non-uniform surfaces (including solid-electrolyte interfaces) or the catalytic action of impurities.[30] However, such inhomogeneities may lead to uneven deposition that could later be magnified by the instabilities studied in this work.

In summary, this work identifies two criteria for growth instability during electrodeposition. The first criterion is defined in terms of the ratio, L/L^*, between the length scale of the features of the deposit and the characteristic length scale that is a function of the material parameters of the system. This ratio is also identified as the second Damköhler number associated with the length scale of the features of the deposit, and the criterion applies when the current is sufficiently small. The second criterion is based on the same ratio, which we termed as the modified Damköhler number, but with the exchange current density in L^* replaced by the far-field average current density. This criterion applies for instabilities arising from the large overpotentials required to maintain large current densities, which makes the nonlinearity of the exponential term in the Butler–Volmer equation important. This instability is also influenced by the roughness of the surface, and thus the relevant length scale is the feature size of the deposits. When sufficiently strong (i.e., the numbers are much greater than unity), both of these two instability mechanisms would increase surface roughness, which would trigger a positive feedback loop and eventually lead to runaway dendritic growth. However, if the deposition surface is nearly flat (as compared with the respective characteristic length scales), the roughness increase will be overrun by the growing front. Therefore, our results suggest that unstable electrodeposition can be suppressed by favoring relatively homogenous initial conditions, such as those resulting from high nucleation densities, and also by controlling kinetics by lowering the exchange current density and increasing the ionic conductivity.

Acknowledgments

The authors would like to thank H.-C. Yu for critical reading of the manuscript. This work was supported as part of the Joint Center for Energy Storage Research, an Energy Innovation Hub funded by the U.S. Department of Energy, Office of Science, Basic Energy Sciences. Additionally, this research used resources of the National Energy Research Scientific Computing Center, a DOE Office of Science User Facility supported by the Office of Sciences of the U.S. Department of Energy under Contract No. DE-AC02-05CH11231.

Supplementary material

The supplementary material for this article can be found at https://doi.org/10.1557/mrc.2017.38

https://doi.org/10.1557/mrc.2017.38 Published online by Cambridge University Press

References

1. Y.D. Gamburg and G. Zangari: *Theory and Practice of Metal Electrodeposition.* (Springer, New York, 2011).
2. J.L. Barton and J.O. Bockris: The electrolytic growth of dendrites from ionic solutions. *Proc. R. Soc. A Math. Phys. Eng. Sci.* **268**, 485–505 (1962).
3. C. Monroe and J. Newman: Dendrite growth in lithium/polymer systems. *J. Electrochem. Soc.* **150**, A1377 (2003).
4. R. Akolkar: Modeling dendrite growth during lithium electrodeposition at sub-ambient temperature. *J. Power Sources* **246**, 84–89 (2014).
5. F. Ding, W. Xu, G.L. Graff, J. Zhang, M.L. Sushko, X. Chen, Y. Shao, M. H. Engelhard, Z. Nie, J. Xiao, X. Liu, P.V. Sushko, J. Liu and J.-G. Zhang: Dendrite-free lithium deposition via self-healing electrostatic shield mechanism. *J. Am. Chem. Soc.* **135**, 4450–4456 (2013).
6. N. Goldenfeld: Dynamics of dendritic growth. *J. Power Sources* **26**, 121–128 (1989).
7. L.-G. Sundström and F.H. Bark: On morphological instability during electrodeposition with a stagnant binary electrolyte. *Electrochim. Acta* **40**, 599–614 (1995).
8. S. DeWitt, N. Hahn, K. Zavadil and K. Thornton: Computational examination of orientation-dependent morphological evolution during the electrodeposition and electrodissolution of magnesium. *J. Electrochem. Soc.* **163**, A513–A521 (2015).
9. W. Xu, J. Wang, F. Ding, X. Chen, E. Nasybulin, Y. Zhang and J.-G. Zhang: Lithium metal anodes for rechargeable batteries. *Energy Environ. Sci.* **7**, 513–537 (2014).
10. Y. Okajima, Y. Shibuta and T. Suzuki: A phase-field model for electrode reactions with Butler–Volmer kinetics. *Comput. Mater. Sci.* **50**, 118–124 (2010).
11. L. Liang and L.-Q. Chen: Nonlinear phase field model for electrodeposition in electrochemical systems. *Appl. Phys. Lett.* **105**, 263903 (2014).
12. D.R. Ely, A. Jana and R.E. García: Phase field kinetics of lithium electrodeposits. *J. Power Sources* **272**, 581–594 (2014).
13. B. Orvananos, T.R. Ferguson, H.-C. Yu, M.Z. Bazant and K. Thornton: Particle-level modeling of the charge–discharge behavior of nanoparticulate phase-separating Li-ion battery electrodes. *J. Electrochem. Soc.* **161**, A535–A546 (2014).
14. N. Moelans, B. Blanpain and P. Wollants: Quantitative analysis of grain boundary properties in a generalized phase field model for grain growth in anisotropic systems. *Phys. Rev. B* **78**, 24113 (2008).
15. J.W. Cahn and J.E. Hilliard: Free energy of a nonuniform system. I. Interfacial free energy. *J. Chem. Phys.* **28**, 258–267 (1958).
16. S.M. Allen and J.W. Cahn: A microscopic theory for antiphase boundary motion and its application to antiphase domain coarsening. *Acta Metall.* **27**, 1085–1095 (1979).
17. J.N. Chazalviel: Electrochemical aspects of the generation of ramified metallic electrodeposits. *Phys. Rev. A* **42**, 7355–7367 (1990).
18. C. P. Nielsen and H. Bruus: Morphological instability during steady electrodeposition at overlimiting currents. *Phys. Rev. E* **92**, 052310 (2015).
19. H.-C. Yu, H.-Y. Chen and K. Thornton: Extended smoothed boundary method for solving partial differential equations with general boundary conditions on complex boundaries. *Model. Simul. Mater. Sci. Eng.* **20**, 75008 (2012).
20. H.S. Fogler: *Elements of Chemical Reaction Engineering* (Prentice Hall, Upper Saddle River, NJ, 2006).
21. S.-I. Lee, U.-H. Jung, Y.-S. Kim, M.-H. Kim, D.-J. Ahn and H.-S. Chun: A study of electrochemical kinetics of lithium ion in organic electrolytes. *Korean J. Chem. Eng.* **19**, 638–644 (2002).
22. S.J. Banik and R. Akolkar: Suppressing dendrite growth during zinc electrodeposition by PEG-200 additive. *J. Electrochem. Soc.* **160**, D519–D523 (2013).
23. C. Wagner: Theoretical analysis of the current density distribution in electrolytic cells. *J. Electrochem. Soc.* **98**, 116 (1951).
24. A. Arneodo, F. Argoul, Y. Couder and M. Rabaud: Anisotropic Laplacian growths: from diffusion-limited aggregates to dendritic fractals. *Phys. Rev. Lett.* **66**, 2332–2335 (1991).
25. O. Crowther and A.C. West: Effect of electrolyte composition on lithium dendrite growth. *J. Electrochem. Soc.* **155**, A806 (2008).
26. Y. Zhang, J. Qian, W. Xu, S.M. Russell, X. Chen, E. Nasybulin, P. Bhattacharya, M.H. Engelhard, D. Mei, R. Cao, F. Ding, A.V. Cresce, K. Xu and J.-G. Zhang: Dendrite-free lithium deposition with self-aligned nanorod structure. *Nano Lett.* **14**, 6889–6896 (2014).
27. B.L. Mehdi, J. Qian, E. Nasybulin, C. Park, D.A. Welch, R. Faller, H. Mehta, W.A. Henderson, W. Xu, C.M. Wang, J.E. Evans, J. Liu, J.-G. Zhang, K.T. Mueller and N.D. Browning: Observation and quantification of nanoscale processes in lithium batteries by operando electrochemical (S)TEM. *Nano Lett.* **15**, 2168–2173 (2015).
28. A.J. Leenheer, K.L. Jungjohann, K.R. Zavadil, J.P. Sullivan and C.T. Harris: Lithium electrodeposition dynamics in aprotic electrolyte observed in situ via transmission electron microscopy. *ACS Nano* **9**, 4379–4389 (2015).
29. D.A. Cogswell: Quantitative phase-field modeling of dendritic electrodeposition. *Phys. Rev. E* **92**, 11301 (2015).
30. J. Steiger, D. Kramer and R. Mönig: Mechanisms of dendritic growth investigated by in situ light microscopy during electrodeposition and dissolution of lithium. *J. Power Sources* **261**, 112–119 (2014).

https://doi.org/10.1557/mrc.2017.38 Published online by Cambridge University Press